



Engineered TiO₂ photocatalyst – Mechanism, kinetics, and application in dye removal: A review

Ayushman Bhattacharya and Ambika Selvaraj*

Department of Civil Engineering, Indian Institute of Technology Hyderabad, Hyderabad-502 285, Telangana, India

E-mail: ambika@ce.iith.ac.in

Manuscript received online 02 December 2020, accepted 23 December 2020

Rapid industrialization and escalating urbanization generate a huge quantity of wastewater with a continuous surge in the wide variety of organic pollutants. Heterogeneous photocatalysis, an advanced oxidation process is highly efficient, robust, sustainable, economical, and effective treatment technology for the detoxification of dyes from the aqueous phase with strict adherence to the green chemistry principle. Modification and development of an advanced photocatalytic system for macroscale industrial application require deeper cognizance of the mechanism and kinetics of charge transfers involved in photocatalytic reaction for the treatment of industrial dye effluents. Therefore, this review aims to detail the kinetic model and compiles the photodegradation of various dyes using TiO₂ as the photocatalyst. Correspondingly, the present study recapitulates the application of different dopants and co-dopants along with their synthesis method in enhancing the TiO₂ photocatalytic efficiency for dye removal. This paper provides complete information on photocatalysis which can be used for the effective degradation of textile dyes from an aqueous system.

Keywords: Photocatalysis, dye removal, titanium dioxide.

Introduction

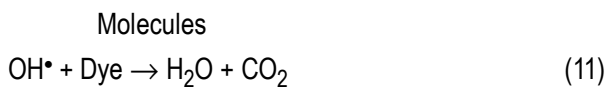
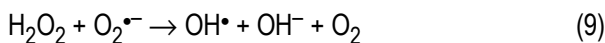
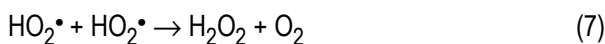
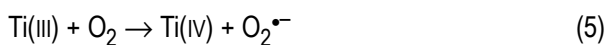
Unprecedented advancement along with the augmented population level and brisk growth of industries are the major factors responsible for the deterioration of the water quality and thereby inducing massive devastation to the aquatic system. Aquatic species pose a threat due to the ejection of dye concentrated industrial effluents. Dyes are the unsaturated organic compound that possesses a complex structure and exhibits recalcitrant, xenobiotic, and carcinogenic nature. Therefore, the degradation of dyes is a major challenge and an emerging environmental concern¹. To overcome the drawbacks associated with conventional treatment techniques like high cost, higher sludge generation, and treatment sensitivity, the advanced oxidation process (AOP) is adopted due to its higher efficiency and a broader range of applications in the domain of wastewater and water treatment. AOP has the potential to oxidize either partly or completely the toxic organic chemicals² by generating the radicals under ambient conditions for complete mineralization of dyes as organic pollutants into carbon dioxide and water³. The application of semiconductor particles as photocatalysts

has significant potential in the photodegradation of a wide variety of textile dyes (Zhang *et al.*, 2012). AOP is an emerging field in wastewater treatment and many researchers are exploring the synthesis and evaluation of novel photocatalysts but there is a lack of assessment related to its advancement⁴. Therefore, this review paper epitomizes the mechanisms, reaction kinetics, governing parameters, and efficacy of various metallic and non-metallic dopants and co-dopants with TiO₂ for dye removal in chronological order.

Mechanism of photocatalytic reactions

The initiation of photocatalytic reaction occurs by irradiation of photon ($h\nu$) having energy greater than or equal to the bandgap energy level (E_g) of the photocatalyst resulting in excitation of electrons (e^-) to the conduction band and generation of holes in the valence band. The generated electrons and holes take part in redox reactions after migrating to the photocatalyst surface with various groups adsorbed on the catalyst surface⁵, resulting in the generation of hydroxyl (OH^\bullet), hydroperoxyl (HO_2^\bullet) and superoxide ($O_2^{\bullet-}$) radicals that oxidize the organic contaminants and inactivates

microorganisms, bacteria, and viruses⁶. The efficiency of photocatalytic reactions can be improved by reducing the bandgap of TiO₂ through chemical modification, thereby enhancing the TiO₂ to work under visible light. The detailed mechanism of photocatalytic reactions for degradation of dyes molecules under the UV-Visible irradiation as illustrated in Fig. 2 are as follows^{4,7,8}.



Kinetics

(A) Adsorption kinetics:

Catalyst fractional site (β_{fs}) is defined as the ratio of the quantity of substrate adsorbed onto the catalyst surface ($Q_{\text{adsorption}}$) to the maximum amount of molecules that can be adsorbed onto a gram of catalyst (Q_{max})⁸.

$$\text{Catalyst fractional site } (\beta_{fs}) = \frac{Q_{\text{adsorption}}}{Q_{\text{max}}} \quad (13)$$

$$\text{where, } Q_{\text{adsorption}} = \frac{C_{\text{in}} - C_{\text{eq}}}{C_{\text{cat}}}, \quad Q_{\text{max}} = \frac{C_{\text{in}}}{C_{\text{cat}}}$$

C_{in} = initial concentration of the substrate (mol/L),

C_{eq} = equilibrium concentration of the substrate (mol/L),

C_{cat} = amount of catalyst per unit amount of solution (g/L).

The rate of the adsorption on the catalyst surface (r_1) is directly proportional to the concentration of substrate and the fractional free available catalyst sites.

$$r_1 = k_1 \times C_{\text{eq}} \times (1 - \beta_{fs}) \quad (14)$$

The rate of the desorption site (r_{-1}) depends on the coverage catalyst surface

$$r_{-1} = k_{-1} \times \beta_{fs} \quad (15)$$

Under equilibrium condition,

Rate of adsorption = Rate of desorption

$$k_1 \times C_{\text{eq}} \times (1 - \beta_{fs}) = k_{-1} \times \beta_{fs} \quad (16)$$

$$\beta_{fs} = \frac{k_1 \times C_{\text{eq}}}{k_{-1} + k_1 \times C_{\text{eq}}}$$

$$\beta_{fs} = \frac{K_{\text{ads}} \times C_{\text{eq}}}{1 + K_{\text{ads}} \times C_{\text{eq}}} \quad (17)$$

$$K_{\text{ads}} = \text{Langmuir adsorption constant} = \frac{k_1}{k_{-1}}$$

Substituting eq. (17) in eq. (13), we get

$$Q_{\text{adsorption}} = \frac{Q_{\text{max}} \times K_{\text{ads}} \times C_{\text{eq}}}{1 + K_{\text{ads}} \times C_{\text{eq}}}$$

$$\frac{C_{\text{eq}}}{Q_{\text{adsorption}}} = \frac{1}{Q_{\text{max}} K_{\text{ads}}} + \frac{C_{\text{eq}}}{Q_{\text{max}}} \quad (18)$$

(B) Photochemical kinetics:

The photocatalytic reaction eventuates through four stages: (i) migration of reactant to the catalyst surface from the bulk solution, (ii) evolution of intermediate species due to adsorption of reactant onto the catalyst surface, (iii) chemical degradation followed by desorption of product, and (iv) conveyance of transformed product back to the bulk liquid phase⁹. According to Phan *et al.*⁹, Langmuir-Hinshelwood model can be used for the computation of steps (ii) and (iii).

Rate of photocatalytic degradation of contaminant,

$$r = \frac{dc}{dt} = - \frac{k_0 KC}{1 + KC} \quad (19)$$

k_0 = reaction rate constant,

C = concentration of organic contaminants,

K = adsorption coefficient of the reactant on the catalyst,

t = reaction time.

$$\int_{C_0}^{C_t} \frac{1 + KC}{KC} dc = -k \int_0^t dt \quad (20)$$

C_0 = organic contaminant concentration at $t = 0$,

C_t = organic contaminant concentration at time t .

Solving the integration, we will get,

$$\begin{aligned} \ln C_t - \ln C_0 + KC_t - KC_0 &= -k_0 K t \\ \ln C_t + KC_t &= \ln C_0 + KC_0 - k_0 K t \end{aligned} \quad (21)$$

Trial and error approach can be used to calculate model parameters like k_0 and K .

(i) If the magnitude of KC is very small, then eq. (19) can be written as a pseudo-first order reaction equation which is as follows:

$$r = \frac{dc}{dt} = -k_0 KC = -k_1 C \quad (22)$$

(ii) If KC is greater than 1, eq. (19) can be simplified to the pseudo-zeroth order reaction equation which is as follows. When the concentration of organic pollutant is high then a pseudo-zeroth order equation is used to calculate the degradation rate¹⁰.

$$r = \frac{dc}{dt} = -k_0$$

$$\int_{C_0}^{C_t} dc = -k \int_0^t dt$$

$$C_t = C_0 - k t \quad (23)$$

Inverting the eq. (19), we get

$$\frac{1}{r} = \frac{1}{k_0} + \frac{1}{k_0 KC} \quad (24)$$

Plotting $1/r$ vs $1/c$, a straight line will be attained and its intercept gives the rate constant (k_0) and its slope determines the adsorption coefficient value (K). According to Phan *et al.*⁹, Beer-Lambert law can be used for the calculation of the propagation of intensity of light through the semiconductor.

$$I = I_0 e^{-\alpha z} \quad (25)$$

where I_0 = intensity of light at the surface of the catalyst layer,

I = intensity of light inside a semiconductor,

α = extinction coefficient,

z = depth of penetration of light inside the semiconductor.

Governing parameters

(a) pH:

Photocatalytic degradation rates can be significantly influenced by varying pH of the solution. The point of zero charge (PZC) is a phenomenon when the surface charge on the photocatalyst is zero or neutral. For TiO_2 , PZC occurs at pH 6.8. At PZC, due to the absence of attraction/repelling force, there is a minimal reaction between the contaminants and photocatalyst in the water. The below reaction signifies that the adsorbent surface will be positively charged when the pH is less than 6.8, fostering the anion attraction and cation repulsion in the water. Similarly, when the pH is more than 6.8, the adsorbent surface becomes negatively charged and stimulates cation attraction and anion repulsion in the water¹¹.



(b) Light intensity:

Radiation of light initiates the generation of electrons and holes for the redox reaction and its intensity influences the amount of absorption of photons by photocatalyst which ultimately governs the rate of photocatalytic reaction³. The reaction rate is directly proportional to the intensity of light (I_0).

$$\frac{dc}{dt} = r \propto (I_0)^n \quad (28)$$

A linear relationship exists between reaction rate and intensity of light at a lower intensity, following the first-order kinetics ($n = 1$) leading to the generation of electrons and holes with negligible recombination between them. With further increase in the light intensity, reaction rate becomes directly proportional to the square root of the light intensity following half order kinetics ($n = 1/2$) ultimately lowering the reaction rate due to the occurrence of electron-hole pair recombination. At a very high intensity, the reaction rate follows zero order ($n = 0$) ensuing that the reaction rate is independent of the intensity of light because, at a higher intensity, the rate-limiting step is achieved i.e generation of $\text{O}_2^{\bullet-}$ takes place due to the migration of electrons from the catalyst surface to the aqueous solution^{3,4,8}.

(c) *Photocatalyst loading:*

Ajmal *et al.*¹¹ reported that photocatalytic reaction rate increases with the increase in photocatalyst loading initially because of higher availability of active sites for adsorption and degradation of dye molecules and also the interaction between the particles increases causing deactivation of activated dye molecules due to collision with ground state TiO₂ particles but with further intensification in the photocatalyst loading, reaction rate declines due to agglomeration of TiO₂ particles and inhibition of light penetration because of solution opacity.

(d) *Effect of initial dye concentration:*

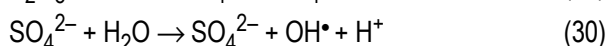
The rate of photocatalytic degradation increases with the increase in initial dye concentration but excessive higher dye concentration fosters the solution opacity that lowers the light penetration inside the reactor and as a result, fewer photons reach the catalyst surface resulting in a decrement of photocatalytic degradation rate⁴. Furthermore, higher contaminant concentration will block the active sites of the photocatalyst, thereby suppressing the OH[•] production rendering the process inefficient¹¹.

(e) *Influent flow rate:*

A higher flow rate reduces the retention time and decreases the reaction rate. However, a higher flow rate can ameliorate the reaction rate by enhancing the diffusion between the contaminant and TiO₂ photocatalyst. But the effect was more dominant in the case of reduced retention time causing the lowering of overall treatment efficiency³.

(f) *Effect of oxidants:*

Konstantinou and Albanis¹² have reported that the addition of H₂O₂ and S₂O₈²⁻ facilitates the photo-oxidation of the various dyes. The reaction of these species with the photogenerated electrons leads to the formation of reactive radical intermediate species (SO₄²⁻ and OH[•]) which exhibit a dual role: a strong oxidizing agent themselves and as electron scavengers, thus impeding the recombination of electron and holes at the photocatalyst surface. The reaction is as follows:



Strategies for enhancing photocatalytic activity of TiO₂

(i) *Metal dopants:*

Two types of metals namely transition metal and noble metal have been mainly discussed in this study for the doping of TiO₂. Al-Mamun *et al.*¹³ have investigated the performance of various types of transition metals like vanadium (V), zinc (Zn), manganese (Mn), nickel (Ni), chromium (Cr) and cobalt (Co) for degradation of dyes and have observed that thermal instability occurs due to the doping of transition metal in anatase phase of TiO₂. Besides, the investigation revealed that for the removal of Congo Red dye, Cr doped TiO₂ (3 mol%) yielded the highest photodegradation i.e. 61% due to its escalated charge carriers followed by 26% and 2.61% photodegradation with Co and V doped TiO₂ respectively, revealing a lower efficiency of V doped TiO₂ due to poisonous effect. In the photocatalytic degradation of Rhodamine B, photocatalytic activity was found to be declined in Mn²⁺ and Ni²⁺ doped TiO₂ whereas higher photocatalytic activity having a removal efficiency of about 98.7% was observed in Zn²⁺ doped TiO₂ within 50 min at optimum dopant concentration of 0.372 wt.% Zn²⁺ synthesized at the 550°C calcination temperature due to reduced rate of electron-hole pair recombination and higher ionic radii of Zn²⁺. Noble metal dopants that can improve the photocatalytic performance of TiO₂ are Au, Pt, Ag, and Pd due to charge transfer, electron transfer, and lower bandgap¹³. Ali, 2018 carried out an experiment for the degradation of Rhodamine B using platinum doped TiO₂ (Pt/TiO₂) photocatalyst of different loadings i.e. 1, 3, 5, and 10 wt.% under visible light. The result showed 99.5% degradation efficiency was achieved in 90 min for Rhodamine B with 5 wt.% platinum loading inferring degradation efficiency escalates with an increase in platinum loading whereas in the case of 10 wt.% platinum loading, degradation efficiency declines because a further increase in platinum loading blocks the light penetration.

(ii) *Non-metal dopants:*

Non-metals like nitrogen, carbon, sulphur, chlorine, and fluoride are mostly used for the modification of TiO₂ photocatalytic properties¹³. Putri *et al.*¹⁴ studied the effect of carbon nitrogen co-doped TiO₂ photocatalyst (C-N-TiO₂) prepared using sol-gel method for the degradation of violet-3B

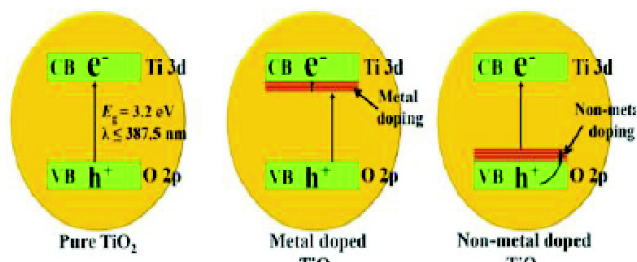


Fig. 1. Band gap of pure and modified TiO_2 photocatalyst (Low *et al.*, 2017).

these dyes on the modified fabric due of their cationic nature whereas degradation efficiency of about 95.4% for methyl blue was achieved after 180 min of treatment because of weaker adsorption of methyl blue dye on the modified fabric due to its anionic nature.

(iii) Metal-nonmetal dopants:

Various metal-nonmetal co-dopants used in the modification of TiO_2 photocatalyst for removal of extensive variety of dyes are Pd-Ni, Gd-N, La-N, Bi-N, Mn-P, Mn-N, Y-N, Cu-

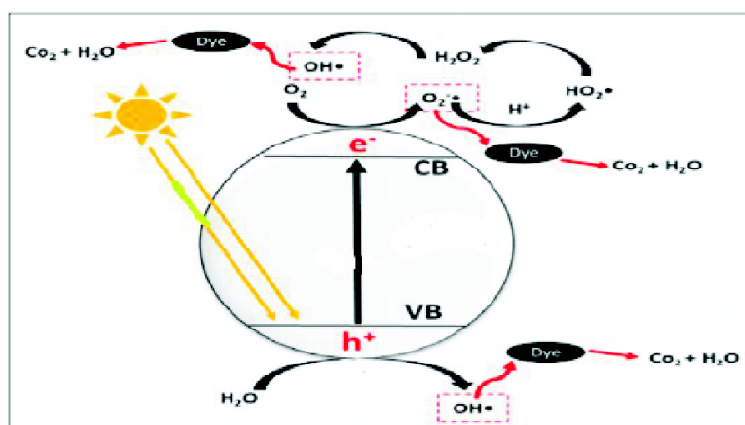


Fig. 2. Schematic illustration of photocatalytic degradation of dye molecule (Chiam *et al.*, 2020)¹⁷.

dye under visible halogen lamp (100 W) illumination. The analysis revealed that percentage removal for violet-3B dye increases up to 83% in 180 min when catalyst concentration is increased from 0.05 to 0.3 g/L because active sites increased but with further increase in catalyst concentration from 0.3 to 1.2 g/L, degradation efficiency declines because of an increase in turbidity resulting in the blockage of light penetration. Besides, increasing the initial concentration of violet-3B dye from 5 to 30 mg/L lowers the degradation rate due to an increase in solution opacity. Cao *et al.*¹⁵ demonstrated the degradation of Rhodamine B, Methylene blue and Methyl Orange dye using chlorine doped TiO_2 coated fabric. The modified fabric was placed inside the three 100 mL solutions comprising of Rhodamine B, Methylene blue, and Methyl Orange dye respectively and each having a concentration of 20 mg/L. It was observed that after 50 min, 95.2% and 96% degradation efficiency for Rhodamine B and Methylene blue was achieved because of strong adsorption of

N, Fe-N, Mo-C. Mancuso *et al.*, 2020 synthesized the iron nitrogen co-doped TiO_2 photocatalyst (Fe-N-TiO_2) through sol-gel method for the decolorization and mineralization of Acid Orange 7 azo dye under visible light illumination (10 W). Experimentation revealed that after 60 min of treatment, iron nitrogen co-doped TiO_2 photocatalyst demonstrated 90% decolorization and 83% mineralization because of enhanced photocatalytic activity due to lower bandgap (2.7 eV) and reduced electron-hole recombination. Alim *et al.*¹⁶ investigated the performance of nickel phosphorus co-doped TiO_2 photocatalyst (N-P-TiO_2) synthesized by sol gel method for the eradication of Methylene blue dye under visible light irradiation (400 W). It was found that optimum photocatalyst loading for the effective degradation for Methylene blue (20 mg/L) is 0.1 g/L. Also, higher degradation of dye was achieved at pH 10 due to negative zeta potential of photocatalyst causing increased electrostatic attraction of cationic nature of dye molecule on its negative surface. N-P-TiO_2 comprising of

0.25% and 0.75% (in wt.) nickel and phosphorus showed 99.5% dye degradation within 75 min due to lower bandgap (2.6 eV) and smaller size of N-P-TiO₂ photocatalyst (4.5 nm) with higher surface area facilitating in higher adsorption of dye molecule.

Conclusion

Heterogeneous photocatalysis is a sustainable method and is of high research interest in the field of industrial effluent treatment. The performance of heterogeneous photocatalysis is significantly influenced by the various parameters which include initial pollutant concentration, pH, intensity of light, influent flow rate, photocatalyst loading and presence of oxidants. The valence states, band-gap and ionic radius exhibit a strong influence on the photocatalytic degradation rate. When the adsorption coefficient, reactant concentration or both are small, pseudo-first order can be used to estimate the kinetics. In case of higher organic concentration, pseudo-zeroth order can be used to estimate the degradation rate. Modification of TiO₂ using metal and non-metal dopants and co-dopants escalates the dye degradation efficiency. Visible light assisted advanced and composite photocatalyst particles of higher stability and manifesting low energy recovery and reuse need to be investigated for the treatment of complex dyes. Development and modeling of dual purpose photocatalyst should be explored with a major focus on single and multi-electron transfer processes for pollutant removal along with energy/fuel synthesis. Designing and scaling of pilot-scale photocatalytic reactor to the industrial level by coupling with membrane separation processes for the eradication of dyes should also be probed.

References

1. B. Lellis, C. Z. Fávoro-Polonio, J. A. Pamphile and J. C. Polonio, *Biotechnol. Res. Innov.*, 2019, **3**, 275. <https://doi.org/10.1016/j.biori.2019.09.001>.
2. C. R. Holkar, A. J. Jadhav, D. V. Pinjari, N. M. Mahamuni and A. B. Pandit, *J. Environ. Manage.*, 2016, **182**, 351. <https://doi.org/10.1016/j.jenvman.2016.07.090>.
3. H. Zangeneh, A. A. L. Zinatizadeh, M. Habibi, M. Akia and M. Hasnain Isa, *J. Ind. Eng. Chem.*, 2015, **26**, 1. <https://doi.org/10.1016/j.jiec.2014.10.043>.
4. S. Mozia, *Sep. Purif. Technol.*, 2010, **73(2)**, 71. <https://doi.org/10.1016/j.seppur.2010.03.021>.
5. M. N. Subramaniam, P. S. Goh, W. J. Lau, B. C. Ng and A. F. Ismail, "Development of nanomaterial-based photocatalytic membrane for organic pollutants removal. In *Advanced Nanomaterials for Membrane Synthesis and Its Applications*", Elsevier Inc., 2018, Chap. 3, pp. 45-67. <https://doi.org/10.1016/B978-0-12-814503-6.00003-3>.
6. S. Leong, A. Razmjou, K. Wang, K. Hapgood, X. Zhang and H. Wang, *Journal of Membrane Science*, 2014, **472**, 167. <https://doi.org/10.1016/j.memsci.2014.08.016>.
7. G. Boczkaj and A. Fernandes, *Chem. Eng. J.*, 2017, **320**, 608. <https://doi.org/10.1016/j.cej.2017.03.084>.
8. R. Molinari, P. Argurio, M. Bellardita and L. Palmisano, *Comprehensive Membrane Science and Engineering*, 2017. <https://doi.org/10.1016/B978-0-12-409547-2.12220-6>.
9. D. D. Phan, F. Babick, M. T. Nguyen, B. Wessely and M. Stintz, *Chem. Eng. Sci.*, 2017, **173**, 242. <https://doi.org/10.1016/j.ces.2017.07.043>.
10. K. H. Choo, "Modeling Photocatalytic Membrane Reactors, Current Trends and Future Developments on (Bio-) Membranes: Photocatalytic Membranes and Photocatalytic Membrane Reactors", Elsevier Inc., 2018. <https://doi.org/10.1016/B978-0-12-813549-5.00010-4>.
11. A. Ajmal, I. Majeed, R. N. Malik, H. Idriss and M. A. Nadeem, *Royal Society of Chemistry Advances*, 2014, **4**, 37003. <https://doi.org/10.1039/c4ra06658h>.
12. I. K. Konstantinou and T. A. Albanis, *Appl. Catal. B: Environ.*, 2004, **49**, 1. <https://doi.org/10.1016/j.apcatb.2003.11.010>.
13. M. R. Al-Mamun, S. Kader, M. S. Islam and M. Z. H. Khan, *J. Environ. Chem. Eng.*, 2019, **7**. <https://doi.org/10.1016/j.jece.2019.103248>.
14. R. A. Putri, S. Safni, N. Jamarun, U. Septiani, M. K. Kim and K. D. Zoh, *Environ. Eng. Res.*, 2020, **25**, 529. <https://doi.org/10.4491/eer.2019.196>.
15. Z. Cao, T. Zhang, P. Ren, D. Cao, Y. Lin, L. Wang, B. Zhang and X. Xiang, *Catalysts*, 2020, **10**. <https://doi.org/10.3390/catal10010069>.
16. S. A. Alim, T. S. Rao, S. R. Mditana and K. V. D. Lakshmi, *J. Nanostructure Chem.*, 2020, **10**, 211. <https://doi.org/10.1007/s40097-020-00343-z>.
17. S. L. Chiam, S. Y. Pung and F. Y. Yeoh, *Environ. Sci. Pollut. Res.*, 2020, **27**, 5759. <https://doi.org/10.1007/s11356-019-07568-8>.
18. A. Mancuso, O. Sacco, D. Sannino, S. Pragliola and V. Vaiano, *Arab. J. Chem.*, 2020, **13**, 8347. <https://doi.org/10.1016/j.arabjc.2020.05.019>.